Susceptibility of Large Wind Power Plants to Voltage Disturbances – Recommendations to Stakeholders

Roger Alves de Oliveira, *Graduate Student Member*, *IEEE*, and Math H. J. Bollen, *Fellow*, *IEEE*

***Abstract*—Sufficient fault ride-through (FRT) of large wind power plants (WPPs) is essential for the operation security of transmission system. The majority of studies on FRT do not include all disturbances originating in the transmission system or the disturbances irrelevant to the operation security. Based on the knowledge of power quality, this paper provides a guide to stakeholders in different aspects of FRT for wind turbines (WTs) and WPPs. This paper details the characteristics of the most common disturbances originated in the transmission system, how they propagate to the WT terminals, and how they impact the dynamic behavior of a large WPP. This paper shows that the details of the voltage disturbances, not only in the transmission system, but also at the WT terminals, should be taken into consideration. Moreover, a detailed representation or characterization of voltage dips is important for FRT studies, despite that the simplified models used in the literature are insufficient. This paper strongly recommends that distinct events and additional characteristics such as the phase-angle jump and oscillations in the transition segments should be considered in FRT analysis.**

***Index Terms*—Wind power generation, wind farm, power quality, fault ride-through (FRT), low voltage ride-through (LVRT).**

I. Introduction

THE high reliability of power transmission system is to a large extent obtained through the wide application of the $N-1$ criterion in the operation and planning [1]. There are some variations to this principle, especially in planning, but the basic rule is that no loss of a single component should result in the loss of supply to a bulk supply point.

While ensuring that the $N-1$ criterion holds, it is important to consider not only the loss of a major transmission line, but also other consequences of faults that result in the loss. The faults of the transmission system have numerous consequences with potentially adverse effects such as equipment damage and instability, which are generally handled by the protection.

The fault of the transmission system also results in voltage dip over a large geographical area. A consequence beyond the control of the transmission system operator is the behavior of the connected equipment due to the voltage dip. The most serious concern of this paper is the loss of a large amount of production during the fault. Apart from the loss of the faulted transmission line, which is correctly removed by the protection, the power system will also lose production (incorrect operation of the generation plant protection). This could make it difficult to maintain sufficient operation reserves for the $N-1$ criterion. The loss of a large amount of production could be the loss of a large power plant or numerous small production units such as wind turbines (WTs) and wind power plants (WPPs).

Fault ride-through (FRT) generally refers to the ability of production units to remain connected during and after the voltage dip at the transmission level. The term is equivalent to voltage-dip immunity or voltage tolerance that describes the ability of consuming equipment to ride through voltage dips. Also, low voltage ride-through (LVRT) is used to emphasize that not only faults might lead to low voltage at the WT terminals, but other events at the transmission level such as transformer energizing could also result in a short-term reduction of voltage magnitude.

With the significant penetration of wind power, the grid codes require that the WTs remain connected and support the grid during and after voltage dips. In the late 1990s and early 2000s, each transmission system operator (TSO) introduced its own FRT requirement. Reference [2] compares the FRT requirements for TSOs in Denmark [3], [4], Sweden [5], Germany [6], Scotland [7], and Ireland [8] until 2004. In order to permit WT manufacturers to provide more manageable and cost-effective solutions to meet the requirements of grid codes, there is a need for grid code harmonization among TSOs. The national compliance of the FRT requirements has been established in countries with more than one TSO such as Denmark, where Eltra and Elkraft provided a common FRT requirement in 2004 [9]. In 2005, the Federal Energy Regulatory Commission (FERC) in the U.S. included FRT requirements in the interconnection standard FERC-661 [10]. Nordic countries (Sweden, Denmark, Norway, Finland, and Iceland) introduced a common code [11] in 2007 to

Manuscript received: July 30, 2020; revised: November 20, 2020; accepted: March 2, 2021. Date of CrossCheck: March 2, 2021. Date of online publication: April 5, 2021.

This work was supported by the Swedish Energy Agency project (No. 44958-1).

R. A. de Oliveira (corresponding author) and M. H. J. Bollen are with the Electric Power Engineering Group, Luleå University of Technology, Skellefteå, Sweden (e-mail: roger.oliveira@ltu.se; math.bollen@ltu.se).

DOI: 10.35833/MPCE.2020.000543

achieve the adequate operation of the Nordic power system. Moreover, the European Network of Transmission System Operators for Electricity (ENTSO-E) [12] released a harmonized grid code among TSOs from 36 countries in 2012.

The requirements that are considered particularly relevant to large WPPs by ENTSO-E [12] are presented in Fig. 1, and its parameters are given in Table I. These requirements are dependent on the voltage level of the connection point and the size of installation. Table I is applicable to the type D, which is defined by ENTSO-E as power park modules connected at 110 kV or above power grid. A WPP is of type D if its maximum capacity is at or above a threshold specified for each European area: 75 MW for continental Europe and Great Britain, 30 MW for Nordic countries, 10 MW for Ireland and Northern Ireland, and 15 MW for Baltic countries. In general, if the voltage at the connection point is above the curve, the WPP should remain connected and provide reactive power support. On the other hand, the WPP can be disconnected from the main grid if the voltage at the connection point is below the curve. In Table I, U_{ret} is the retained voltage at the connection point during a fault; t_{clear} is the instant when the fault has been cleared; U_{clear} is the voltage at t_{clear}; U_{rec1}, U_{rec2}, t_{rec1}, t_{rec2}, and t_{rec3} specify certain points of the voltage recovery curve after fault clearance.

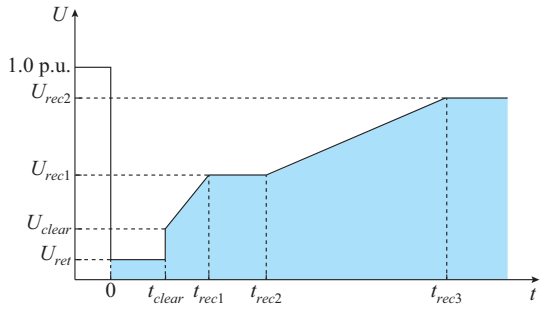

Fig. 1. FRT profile of a power generation module according to ENTSO-E.

TABLE I
PARAMETERS OR FRT CAPABILITY OF WIND PARK MODULES FOR TYPE D

Parameter	Variable	Value
Voltage parameter	U_{ret}	0
	U_{clear}	U_{ret}
	U_{rec1}	U_{clear}
	U_{rec2}	0.85 p.u.
Time parameter	t_{clear}	0.14-0.15 s*
	t_{rec1}	t_{clear}
	t_{rec2}	t_{rec1}
	t_{rec3}	1.5-3.0 s

Note: * means 0.14-0.25 s if system protection and secure operation require so.

The WT manufacturers are required to follow the international standard IEC 61400-21 [13] to test the dynamic response of WTs subjected to voltage dips. The test only considers magnitude, duration, and two types of voltage dips: one symmetrical and another asymmetrical due to a two-phase-to-ground fault. Similarly, IEC 61400-27-1 [14] prescribes a generic set of voltage dips to test the models of WTs in simulation studies.

The FRT requirements and the dynamic response tests are generally limited to two characteristics of voltage dips: magnitude and duration. In real applications, voltage dips present additional characteristics, which are extensively studied in the field of power quality. Such knowledge should be considered in FRT studies. The joint working group C4.110(a) by CIGRE, CIRED, and UIE has proposed a detailed checklist [15] with different properties and characteristics of voltage dips. This checklist divides the voltage waveform into pre-dip, during-dip, and recovery segments. Special emphasis has been placed on the three-phase and occasional non-rectangular characteristics of voltage dips. Similarly, IEEE Standard 1668-2017 [16] defines the minimum voltage dip immunity requirements based on a detailed analysis of real voltage dips. Additional characteristics proposed in [16] include point-on-wave, phase-angle jump, and dip-type.

Although the details of voltage dip characterization have been well-developed in the field of power quality, most studies on FRT consider basic or even incorrect models of voltage dips. Moreover, FRT studies are mostly limited to voltage dips caused by faults. Based on the available knowledge of voltage dip in the field of power quality, this paper provides guidance and recommendations for the research community and other stakeholders on FRT analysis. This paper lists the most common disturbances originated in the transmission system, which should be considered in FRT studies of WPPs, and then considers voltage dips and transients due to various origins such as electrical faults, transformer energizing, capacitor switching, cable switching, loss of major lines or cables, and geomagnetically-induced currents (GICs). Frequency variations are out of scope in this paper. The main contributions are summarized as follows.

1) Disturbances at the WT terminals have a significantly different waveform from those in the transmission system. The former can be more or less severe depending on the disturbance type, the connection to the transmission system, and the collection grid.

2) Detailed representation or characterization of voltage dips and transients is necessary to study their impact on WTs, including additional characteristics such as oscillations at the beginning and the end of the disturbances, phase-angle jumps, and short-term harmonic distortions.

3) It is necessary to provide a more complete set of voltage disturbances based on real power quality measurements, and a set of characteristics and their values, to study and verify the FRT of WTs.

The remainder of this paper is structured as follows. Sections II and III continue the introduction to LVRT, while each section introduces a distinct content. Section II describes the models of voltage dips and disturbances developed in the literature. Section III gives recommendations on the measurement and analysis of voltage dips in and around wind power installations. Section IV gives a detailed overview of the disturbances to be considered in FRT studies, including the recommendations of disturbances and details to be considered in FRT studies. Section V presents the dynamic behavior of a WPP with 42 WTs exposed to the distur-

bances in Section IV. It is shown that the details of the voltage disturbances can have a significant impact. Section VI presents recommendations for FRT requirements in grid codes and connection agreements. Section VII presents recommendations for the research community. Finally, Section VIII concludes this paper.

II. State-of-the-art in Research and Development of LVRT of WPPs

Several works have addressed the FRT of WPPs by voltage dips due to electrical faults. An overview of the types of voltage dips that can be expected at the WT terminals is given in [17]. An analysis of the dynamic behavior of doubly-fed inductor generator (DFIG) with symmetrical and asymmetrical voltage dips is presented in [18] and [19], respectively. References [20] - [22] apply the theory of [17] and study the impact of additional dip characteristics caused by faults. It is concluded in [19] - [22] that the dips caused by symmetric faults lead to overvoltages at the DC-link of the converter and overcurrents in the rotor, both at the beginning of the disturbance, while the dips caused by asymmetric faults could also produce harmonic distortion in the rotor current, in addition to causing overvoltages and overcurrents.

Although [19] - [22] have brought important knowledge regarding the dynamic behavior of WTs with voltage dips, they have not considered the propagation of voltage dips from the transmission level to the WT terminals. The propagation of voltage dips is also not considered in most works related to FRT control strategies. In both dynamic behavior and FRT control studies, there are four methods used to generate voltage dips: ① reducing voltage at the WT terminals [19] - [29]; ② applying faults directly to the terminals [30] - [34]; ③ applying faults in the collection grid [35] - [45]; and ④ considering the propagation from the transmission grid to WT terminals [46] - [52]. There are two different limitations in those models. Some dip types applied to the WTs will never occur in reality at the WT terminals. Some of the fault locations studied do not fall in the realm of FRT but in the realm of the local power system protection. Using overly-simplified or even incorrect models may lead to incorrect conclusions. WPPs may be less tolerant to the faults of the transmission system than expected. Alternatively, WTs may be over-dimensioned and therewith too expensive.

Most works [19] - [45], [47] - [52] only consider electrical faults for FRT analysis. Reference [17] recommends testing the WTs for different origins of disturbances such as transformer energizing and capacitor switching. However, few works evaluate the dynamic behaviors of wind power installations due to events other than faults. Reference [45] has studied the transient behavior of a WPP due to the capacitor switching. Reference [52] discusses the impact of GIC. The transformer energizing is discussed in [53], but only the internal transformers of the WPP are considered. As the WTs are exposed to all types of disturbances from the transmission system, the voltage dips and transients due to other causes should also be studied to guarantee sufficient operation security of the transmission system.

III. Measurement and Analysis of Voltage Dips and Transients in and Around Wind Power Installations

Detailed recordings should be obtained for voltage dips and voltage transients at different locations in WPP. The event at the WT terminals has a significantly different waveform from that in the transmission system. Most studies do not consider this transfer partly due to the lack of available measurement data.

In relation to the recording of voltage dips and other voltage disturbances, data should be collected on the performance of WTs and protection relays in and nearby the WPP. Examples of such data include the voltages during and after voltage dips at the DC side of power-electronic converters, the currents on both sides of the converters, and the values of internal signals that are compared with trip thresholds for the protection relays. These data can be used to extrapolate and model the FTR of a WPP and its WTs during severe voltage dips.

Methods should be developed and agreed internationally, e.g., in CIGRE, IEC or, IEEE context, for a number of additional voltage dip characteristics beyond residual voltage and duration. The following characteristics have been identified starting from the checklist proposed by joint working group (JWG) C4.110 [15]: ① phase-angle jump (between voltages before and during the dip); ② voltage imbalance during the dip; ③ point-on-wave of dip initiation; ④ point-on-wave of voltage recovery, including the multi-step recovery for dips due to two-phase-to-ground and three-phase faults; ⑤ characteristics such as magnitude and frequency of the oscillations in voltage at the beginning and end of the voltage dip; ⑥ characteristics for increased waveform distortion during and after the dip.

The proposals for the first two characteristics can be found in [54] and [55]. The proposals have also been submitted to both IEC and IEEE working groups. The other characteristics require more development and even basic research in some cases [56]. Studies towards broadly acceptable characteristics should be prioritized.

An alternative approach is to create a comprehensive database of voltage dips as they have occurred or may occur at the WT terminals. Such recordings and statistics on the characteristics can be used to verify the FRT at the early design stage of WTs.

IV. Relevant Disturbances

Sufficient FRT of production units is an essential condition for ensuring the operation security of transmission system. The emphasis should be put on the events that affect or potentially affect multiple WPPs or large individual WPPs and those originating in parts of the grid where the $N-1$ criterion holds. This section describes each disturbance in the 155 kV transmission system, and how they propagate to the 33 kV collection grid and the 0.9 kV WT terminals. Section V will present the dynamic behavior of the equivalent WPP with each disturbance.

A. Illustrative WPP with 42 WTs

The disturbances to be considered for FRT, as introduced

in the next sections, are applied to the WPP with 42 WTs in Fig. 2. The DFIG-based WPP consists of 42 WTs of 6.5 MVA connected to the public grid through four 220 MVA (155 kV/33 kV) transformers. Each WT is connected to 33 kV through a 6 MVA transformer. The detailed data of this WPP is available in [57]. The method proposed in [58] to obtain an equivalent of the WPP has been applied to the WPP shown in Fig. 3, where V_{grid}, R_{grid}, and L_{grid} are the equivalents of the public grid for voltage, resistance, and inductance, respectively; R_1, L_1, and C_1 are the equivalents of the collection grid for resistance, inductance, and capacitance, respectively; R_{T1} and L_{T1} are the equivalent resistance and inductance of collection grid transformer, respectively; R_2, L_2, and C_2 are the equivalents of the WPP internal grid for resistance, inductance, and capacitance, respectively; R_{T2} and L_{T2} are the equivalents of resistance and inductance of WT transformers, respectively; R_F, L_F, and C_F are the equivalents of resistance, inductance, and capacitance of the WT filters, respectively; R_G, L_G are the resistance and inductance of DFIG generator, respectively; and n is the number of turbines. Figure 3 shows the equivalent model. The complete model and the equivalent model are compared and they show the same resonant frequency. Appendix A Table AI shows the equivalent parameters for the wind park. The public grid is modeled by its Thévenin equivalent.

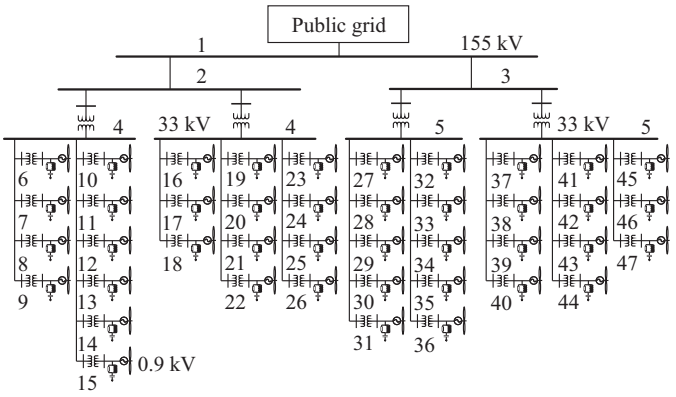

Fig. 2. DFIG-based WPP with 42 WTs.

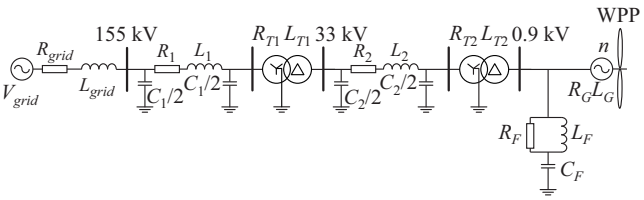

Fig. 3. Equivalent models of transmission system and WPP in Fig. 2.

The DFIG consists of a wound rotor induction generator and an AC/DC/AC based on insulated-gate bipolar transistor (IGBT) pulse width modulation (PWM) converter. The control system uses a torque controller to maintain the speed at 1.2 p.u.. The reactive power produced by the WT is regulated at 0 Mvar. The var/volt control system is based on the model presented in [59]. According to [59], the control functions are segregated into two closed-loop and open-loop controllers. The closed-loop controller includes voltage regulation and power factor control functions. The open-loop controller responds to large disturbances and includes the important protective functions related to the electrical aspects of the WT. A principal feature of the converter is the maximum current of grid-side converter. In this model, the grid-side current is limited to 0.8 p.u. of the nominal current of WT generator. The controllers certainly vary between manufacturers and the details of the controllers are often unavailable. However, the controller used in [59] is a typical controller which is applied in WT. The aim of this paper is not to study the impact of voltage dips on a specific controller, WT, or LVRT technique. Instead, this paper aims to show that the magnitude and duration alone are insufficient when studying the FRT of WTs. The control parameters for the converter are detailed in Appendix A Table AII.

B. Voltage Dips due to Symmetrical Faults in Transmission System

Symmetrical faults occurring at transmission level result in the same voltage drop in all the three phasors. An example of a symmetrical voltage dip is shown in Fig. 4, which presents the waveforms and the corresponding root-mean-square (RMS) voltage for the three voltage levels: 155 kV, 33 kV, and 0.9 kV.

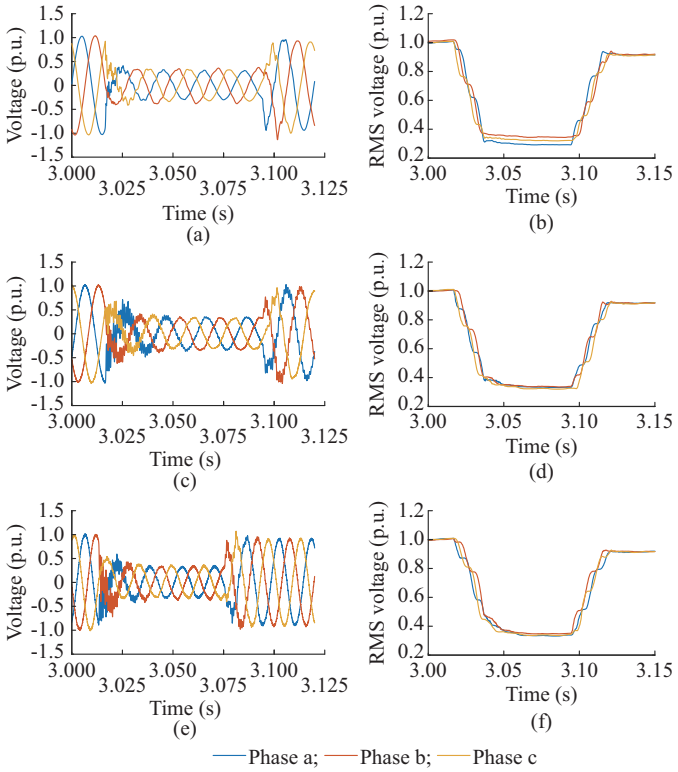

Fig. 4. Symmetrical voltage dip due to a fault at 155 kV. (a) Waveforms measured at 155 kV. (b) RMS voltages measured at 155 kV. (c) Waveforms measured at 33 kV. (d) RMS voltages measured at 33 kV. (e) Waveforms measured at 0.9 kV. (f) RMS voltages measured at 0.9 kV.

The initial voltage drop corresponds to fault initiation. The start of the dip shows a transient caused by the equivalent capacitances and inductances in the transmission system. The transient is amplified and lasts longer after being propagated to lower voltage levels. The amplification is due

to the resonant frequency of the collection grid which is excited by the transient.

The type of voltage dip does not change and its magnitude is almost the same at the three voltage levels. The voltage recovery after the fault is not instantaneous due to load effects, re-energizing of capacitance, and saturation of transformer.

C. Voltage Dips due to Asymmetrical Faults in Transmission System

Asymmetrical faults at transmission level result in unbalanced dips. The dip characteristics such as type or magnitude change when the dip propagates towards the collection grid and WT terminals. An example of an asymmetrical voltage dip caused by a phase-to-ground fault is shown in Fig. 5. The voltage dip of type B at the transmission level changes to type C at the collection grid, and to type D at the WT terminals.

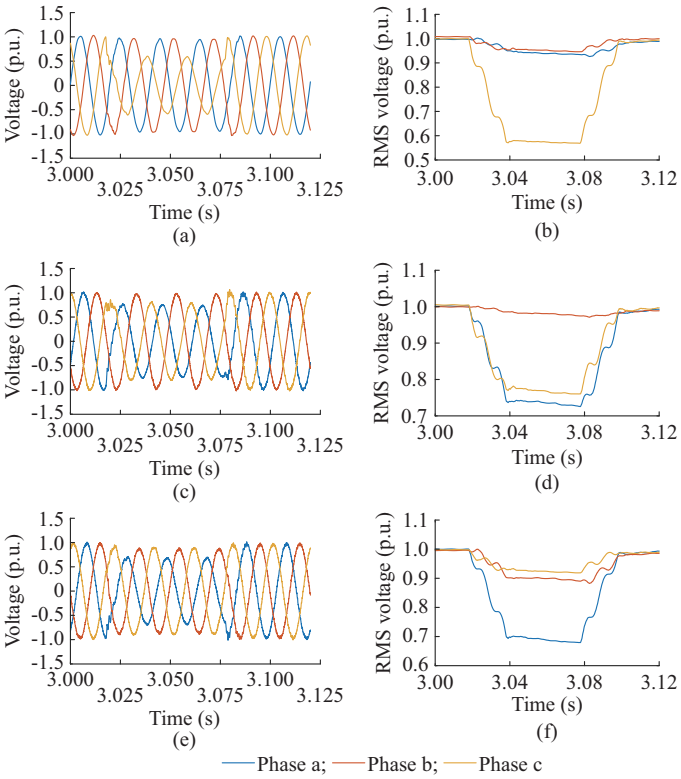

Fig. 5. Asymmetrical voltage dip due to a fault at 155 kV. (a) Waveforms measured at 155 kV. (b) RMS voltages measured at 155 kV. (c) Waveforms measured at 33 kV. (d) RMS voltages measured at 33 kV. (e) Waveforms measured at 0.9 kV. (f) RMS voltages measured at 0.9 kV.

D. Multistage Voltage Dips

During multistage voltage dips, the RMS voltage shows sudden changes. Those changes are related to changes in the fault (developing faults) or changes in the system (fault clearing). A fault on a transmission line is cleared by opening the breakers on both sides of the faulted line. In most cases, this will not happen at exactly the same instant. The result is that the voltage recovery takes place in two stages. This two-stage recovery is very common for the faults in the transmission system. An example of a multistage voltage dip is shown in Fig. 6.

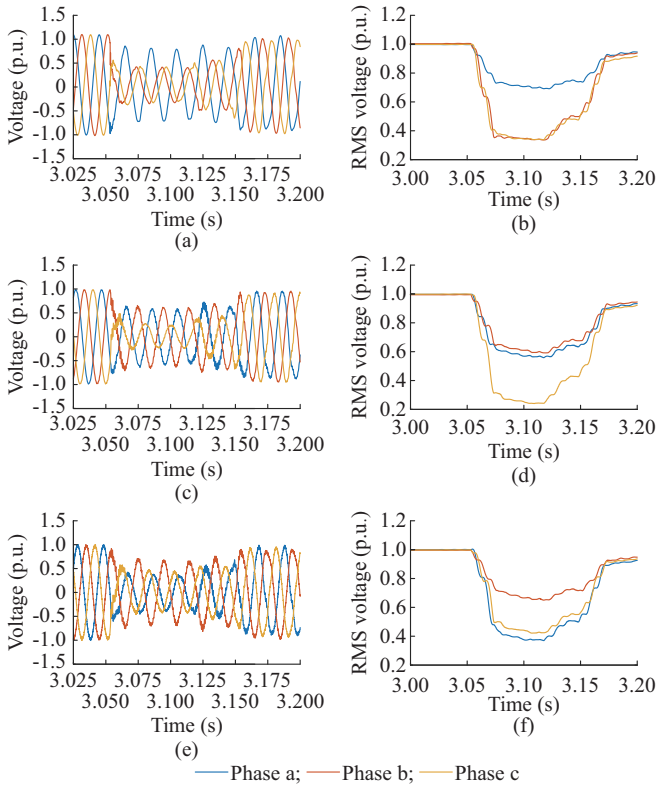

Fig. 6. Multistage voltage dip due to a fault at 155 kV. (a) Waveforms measured at 155 kV. (b) RMS voltages measured at 155 kV. (c) Waveforms measured at 33 kV. (d) RMS voltages measured at 33 kV. (e) Waveforms measured at 0.9 kV. (f) RMS voltages measured at 0.9 kV.

E. Loss of Major Transmission Lines or Cables

The loss of a major transmission line or cable can result in a redirection of power flow and a phase-angle-jump in the voltage. Such a phase-angle-jump is not associated with a voltage dip. Figure 7 shows the propagation of this event from the transmission system to the WT terminals. The loss of the line causes a minor reduction in the RMS voltage, which recovers slowly. The redirection of power flow causes a significant negative phase-angle jump in this case, as shown in Fig. 8(a). The phase-angle jump can also be positive for the loss of another major transmission line as shown in Fig. 8(b).

F. Voltage Dips due to Transformer Energizing

Power transformer energizing can create large flux asymmetries and saturation of the winding cores of transformers, which results in voltage dips with sudden voltage drop and slow voltage recovery. An example of such a voltage dip is shown in Fig. 9.

Each phase experiences a different switching angle in a three-phase transformer, resulting in distinct levels of saturation in each phase. Thus, the drop is different in each phase, resulting in an asymmetrical dip. Similar to the asymmetrical dips caused by faults, the voltage dip changes when it propagates towards the collection grid and WT terminals. The voltage dip due to transformer energizing is associated

with high levels of harmonic distortion, where the levels for even harmonics are much higher than usual. Resonances in the transmission system or between the transmission sytem and the WT terminals can result in even higher levels of harmonic distortion at the WT terminals [60], [61].

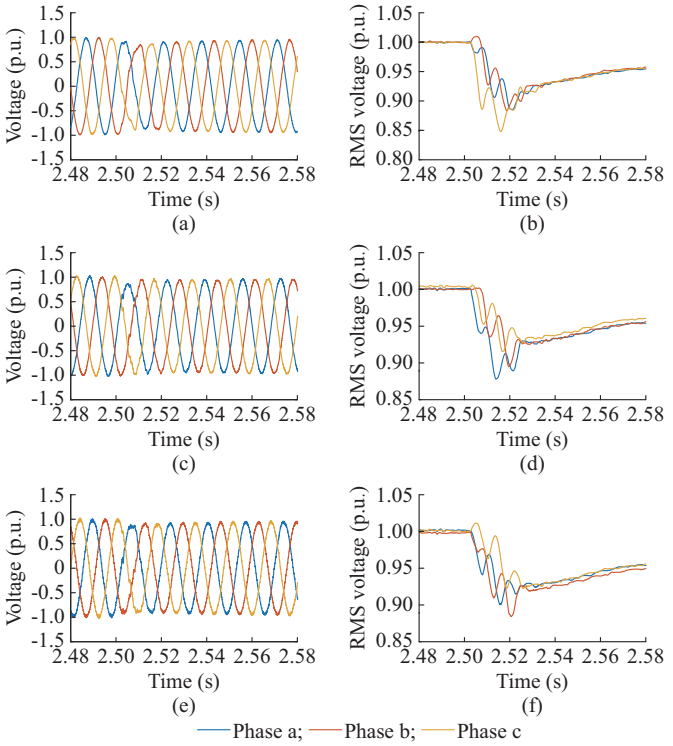

Fig. 7. Loss of a major line at 155 kV. (a) Waveforms measured at 155 kV. (b) RMS voltages measured at 155 kV. (c) Waveforms measured at 33 kV. (d) RMS voltages measured at 33 kV. (e) Waveforms measured at 0.9 kV. (f) RMS voltages measured at 0.9 kV.

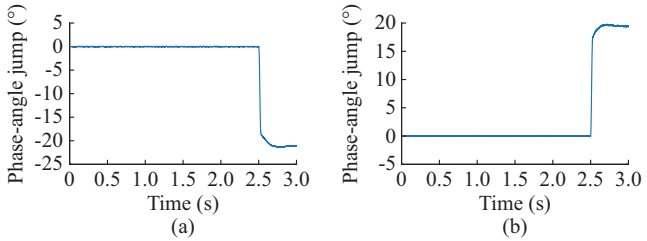

Fig. 8. Phase-angle jump caused by a loss of a major line. (a) Negative phase-angle jump. (b) Positive phase-angle jump.

G. Voltage Transients Due to Capacitor Switching

Voltage transients in power systems are caused mainly by switching actions. The most severe transients are caused by capacitor energizing, while capacitor de-energizing normally only causes a minor transient. Non-synchronized capacitor energizing is worse than the synchronized one. Non-synchronized capacitor energizing at the transmission level results in an oscillation with a frequency in the range of 300-1000 Hz. This oscillation can be amplified by the resonance frequency of the collection grid and/or of the connection between the collection grid and the transmission system. For synchronized switching, the magnitude of the transient is significantly lower, but resonances may still result in dangerous situations.

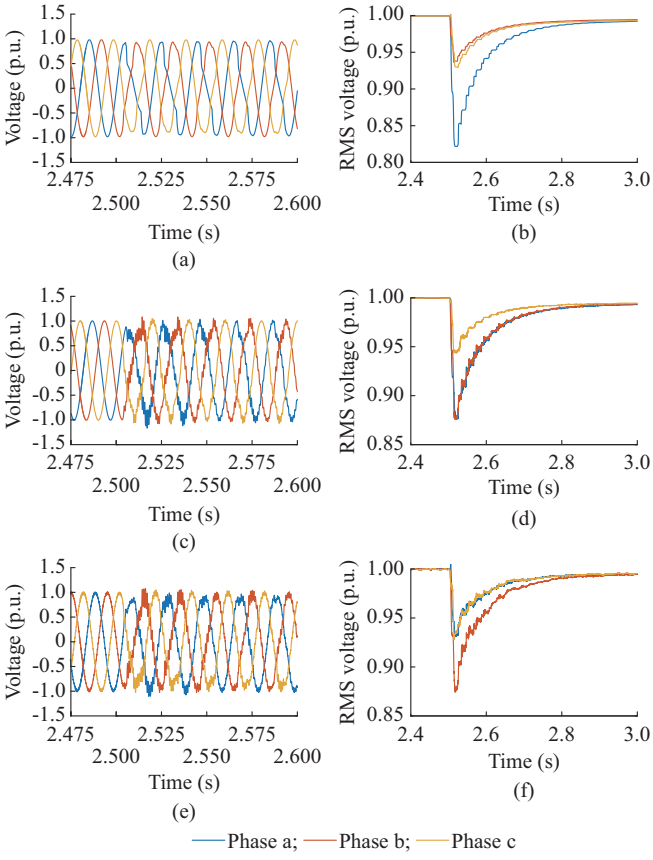

Fig. 9. Transformer-energizing in 155 kV. (a) Waveforms measured at 155 kV. (b) RMS voltages measured at 155 kV. (c) Waveforms measured at 33 kV. (d) RMS voltages measured at 33 kV. (e) Waveforms measured at 0.9 kV. (f) RMS voltages measured at 0.9 kV.

An example of a voltage transient caused by capacitor switching at the transmission level is shown in Fig. 10. Due to the interaction with the capacitance of the collection grid, the transient originating in the transmission system is amplified towards the WT terminals.

H. Voltage Transients due to Cable Switching

Cable switching also results in a voltage transient [62], [63]. Similar to capacitor energizing, its amplitude depends on the moment at which the cable is connected. There is almost no overvoltage transient if the circuit breaker is closed when the voltage is zero at its terminals, but if the connection takes place at peak voltage, the overvoltage is the maximum.

The transient due to cable switching has similar characteristics to the one due to the capacitor switching. For long AC cables at the transmission level, the resonant frequency may be as low as 150 Hz. The cable switching and/or a capacitor switching with other cables located nearby will result in a back-to-back energizing transient. During such a transient, high overvoltage can occur, which can be further amplified by resonances.

Figure 11 presents an example of a voltage transient caused by cable switching. Similar to the transient caused by capacitor switching, the transient due to cable switching is amplified towards the WT terminals.

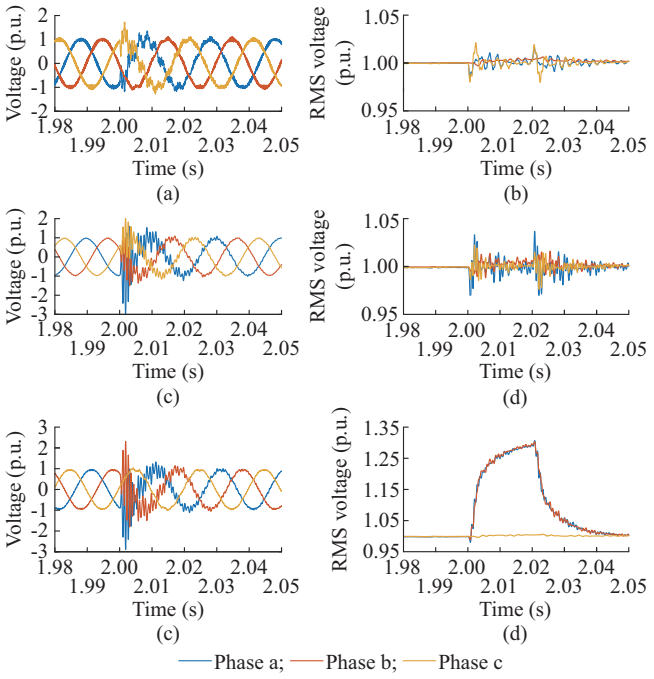

Fig. 10. Voltage transients due to capacitor switching. (a) Waveforms measured at 155 kV. (b) RMS voltages measured at 155 kV. (c) Waveforms measured at 33 kV. (d) RMS voltages measured at 33 kV. (e) Waveforms measured at 0.9 kV. (f) RMS voltages measured at 0.9 kV.

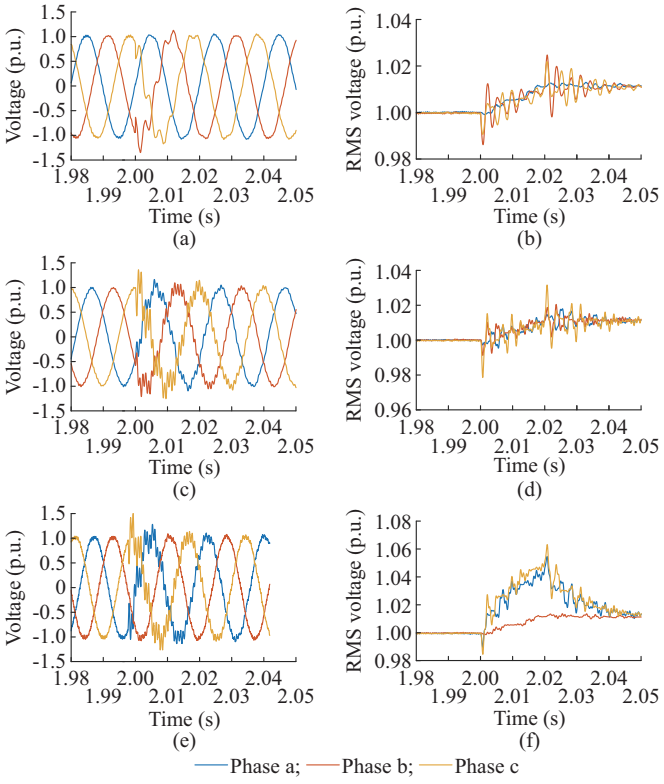

Fig. 11. Voltage transients due to cable switching. (a) Waveforms measured at 155 kV. (b) RMS voltages measured at 155 kV. (c) Waveforms measured at 33 kV. (d) RMS voltages measured at 33 kV. (e) Waveforms measured at 0.9 kV. (f) RMS voltages measured at 0.9 kV.

I. Voltage Dips due to GIC

A GIC event is originated from the interaction between the cloud of charged particles produced by a coronal mass ejection from a solar storm and the magnetic field of the earth [64]. When the coronal mass ejection reaches the Earth's magnetosphere, it affects the geomagnetic field at the Earth's surface. The changes in the geomagnetic field induce slowly varying currents in the conductors of overhead transmission lines, i.e., GICs [65].

GICs can result in transformer saturation and high levels of waveform distortion. The spectrum is expected to be similar to the voltage spectrum during transformer energizing with some differences. The waveform distortion during a GIC event could be much higher as several transformers are saturated at the same time. The waveform distortion may also last much longer. Figure 12 presents an example of a voltage dip due to GIC.

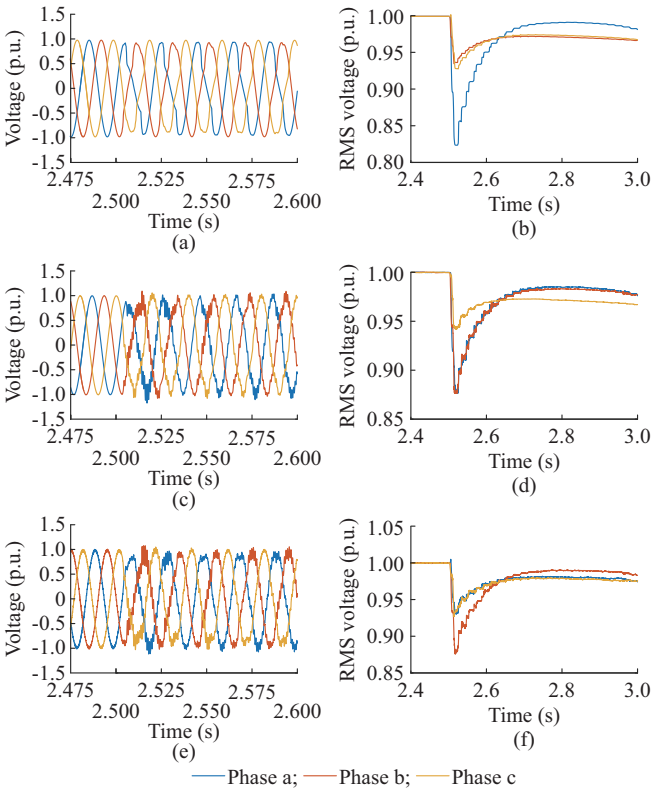

Fig. 12. Voltage dip caused by GIC. (a) Waveforms measured at 155 kV. (b) RMS voltages measured at 155 kV. (c) Waveforms measured at 33 kV. (d) RMS voltages measured at 33 kV. (e) Waveforms measured at 0.9 kV. (f) RMS voltages measured at 0.9 kV.

J. Overview and Considerations for Different Voltage Disturbances

The following points should be considered for different voltage disturbances originating in the transmission system.

1) The voltage dip occurs at the WT terminals, and is not the same as that in the transmission system. The latter is considered in the grid code. The dip at the WT terminals is typically less severe for WTs than that in the transmission system. Oscillations at the beginning and end of the dip related to the resonant frequency of the collection grid, for example, may make the dip more severe at the WT terminals.

2) There is no standard dip for the faults of transmission

system or no standard way of dip propagation from the transmission system to the WT terminals. It is recommended to consider a range of cases with different transmission systems, collection grids, and connections of those collection grids to the transmission system.

3) The phase-angle jumps associated with voltage dips are limited in size for the dips in transmission system consisting of overhead lines. The chosen asymmetrical dips, multistage dips, and transformer-energizing do not present any noticeable phase-angle jump, because these events occur in transmission system consisting of overhead lines.

4) The faults in or near long AC cables at transmission level may result in serious phase-angle jumps that may affect the WT performance. It is the case of the presented symmetrical voltage dip.

5) In addition to the phase-angle jump, during a fault in a cable-dominated grid, there are transients related to the capacitance of the cables. When the dips propagate to the WTs, this transient can be amplified accordingly to the resonance frequency of the collection grid. Because of this, the dips show these high-frequency oscillations at the end of the dips.

6) The point-on-wave of dip initiation can have any value.

7) The point-on-wave of voltage recovery is limited to the values just before the maximum or minimum voltage (due to the reactive characteristics of the transmission system). Voltage recovery takes place in two steps for the dips due to two-phase-to-ground faults and for the dips due to three-phase faults without ground connection. The recovery takes place in three stages for three-phase-to-ground faults.

8) Oscillations may take place in the voltage at the beginning and end of a dip.

9) High levels of voltage distortion, including high levels of even harmonics, can occur after voltage recovery.

V. Verifying FRT of Wind Power Installations

This section presents the dynamic behavior of the equivalent WPP with 42 WTs shown in Figs. 2 and 3. The voltage dips and transients from Section IV have been applied to the equivalent WPP. We apply the measurements to bus 1 in Fig. 2, which represents the public grid at 155 kV. This way, it is considered that the event is measured at 155 kV, which is independent of the event location in the transmission system. The dynamic behavior for different events is assessed in terms of active power, DC-link voltage, and rotor current.

A. Voltage Dips due to Symmetrical Faults

During a symmetrical voltage dip, the stator voltage drops proportionally to the dip magnitude. The stator flux cannot be discontinuous because it is a state variable. After the start of the voltage dip, its magnitude is immediately equal to its previous value and then decreases exponentially with the stator time constant. This results in a rotor overvoltage during the dip initiation. Further, the active power of the grid-side inverter is decreased, and the rotor overcurrent leads to a transient in the DC-link voltage. This transient might be an overvoltage or an undervoltage depending on the phase-angle jump associated with the dip.

Figure 13 shows the dynamic behavior of the equivalent WPP during a symmetrical voltage dip caused by a cable fault from Fig. 4.

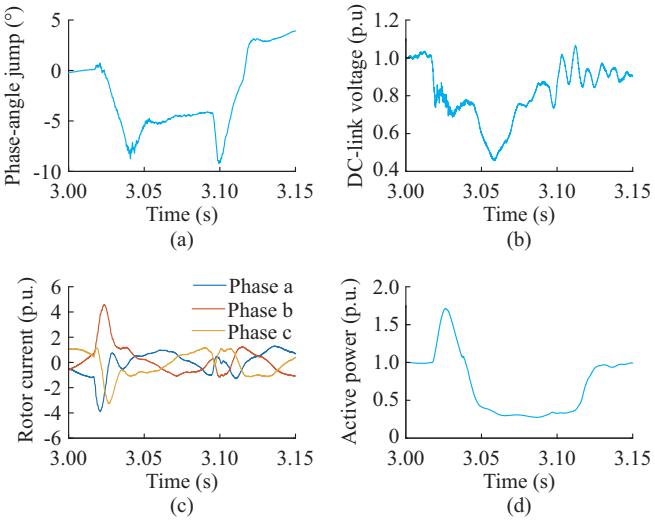

Fig. 13. Dynamic behavior of equivalent WPP during a symmetrical voltage dip caused by a cable fault. (a) Phase-angle jump. (b) DC-link voltage. (c) Rotor current. (d) Active power.

At the beginning of the voltage dip, the DC link shows an undervoltage due to the phase-angle jump associated with the voltage dip. In this specific case, the fault in a transmission cable causes a negative phase-angle jump. An overvoltage is expected for the case with a positive phase-angle jump. At the same instant, there is an overshoot in the rotor current and the active power. The overcurrent in the rotor and the overshoot in the active power reach up to 4 p.u. and 1.6 p.u., respectively.

During the voltage dip, the DC-link voltage is lower than that at the beginning of the dip. The active power is reduced to around 0.4 p.u., proportional to the magnitude of dip. The rotor current shows the waveform distortion during the dip.

During the voltage recovery, the DC-link voltage shows oscillations and it does not reach the pre-dip value immediately. The rotor current is also distorted during recovery. The active power returns to a value close to the pre-dip one.

B. Voltage Dips due to Asymmetrical Faults

During an asymmetrical dip, the negative sequence voltage causes oscillations with a frequency corresponding to the double of the electrical angular velocity of the synchronous reference frame. The rotor voltage component induced by the negative-sequence component of stator flux results in large ripples in the rotor current. This way, the induced rotor voltage could exceed the maximum tolerable voltage of the converter, and the converter could lose control of the rotor current resulting in overcurrent and DC-link overvoltage. The unbalanced voltage dip results in heavy harmonic distortion of rotor current.

Figure 14 presents the results for the dynamic behavior of the equivalent WPP during the asymmetrical dip from Fig. 5. The DC-link voltage shows an undervoltage of 0.8 p.u. at the beginning of the voltage dip. However, the DC-link voltage shows an overvoltage during the voltage dip close to 1.1

p.u.. In the segments during the voltage dip until the recovery, the DC-link voltage oscillates between 0.7 p.u and 1.1 p.u.. The DC-link voltage returns to the pre-dip value after the recovery. The rotor current presents an overcurrent close to 2 p.u. at the beginning of the voltage dip. In addition to the overcurrent, the rotor current shows a high harmonic distortion during the voltage dip. The high distortion and overcurrent disappear after the recovery. The active power presents an overshoot at the beginning of the voltage dip, which reaches 1.1 p.u.. During the dip, the minimum value of the active power is close to 0.9 p.u.. During the recovery, the active power is between 0.9 p.u. and 1 p.u..

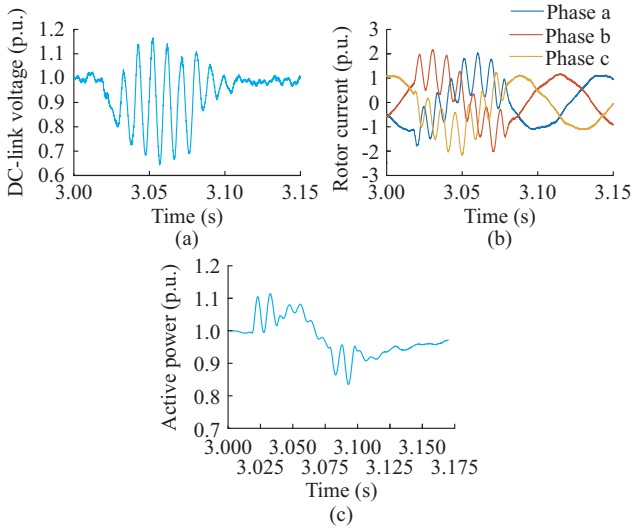

Fig. 14. Dynamic behavior of equivalent WPP during an asymmetrical voltage dip. (a) DC-link voltage. (b) Rotor current. (c) Active power.

C. Multistage Dips

Figure 15 shows the dynamic behavior of the equivalent WPP during a multistage voltage dip from Fig. 6.

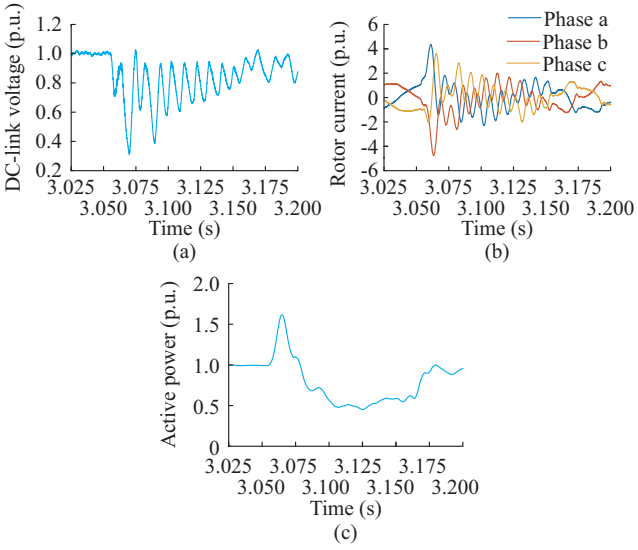

Fig. 15. Dynamic behavior of equivalent WPP during a multistage voltage dip. (a) DC-link voltage. (b) Rotor current. (c) Active power.

The DC-link voltage presents two distinct stages during this multistage dip. At the first stage, it oscillates between 0.4 p.u. and 1 p.u.; at the second stage, it oscillates between 0.7 p.u. and 1 p.u.. The DC-link voltage still shows oscillations after the recovery.

The rotor current shows an overcurrent at the beginning of the voltage dip, which reaches 4 p.u.. During the voltage dip, the rotor current is distorted and shows an overcurrent. The overcurrent is higher at the first stage than that at the second stage. The rotor current is less distorted, but it still shows a harmonic distortion after the voltage recovery.

The active power presents an overshoot close to 1.5 p.u. at the beginning of the voltage dip. During the voltage dip, the active power is reduced proportionally to the magnitude of the dip. As the multistage voltage dip presents two distinct magnitude values during the event, the active power also presents two levels of reduction. During the recovery, the active power oscillates around 1 p.u..

D. Loss of Major Transmission Lines or Cables

Figure 16(a), (c), and (e) presents the results for the dynamic behavior of the equivalent WPP during the loss of a line presented in Fig. 7.

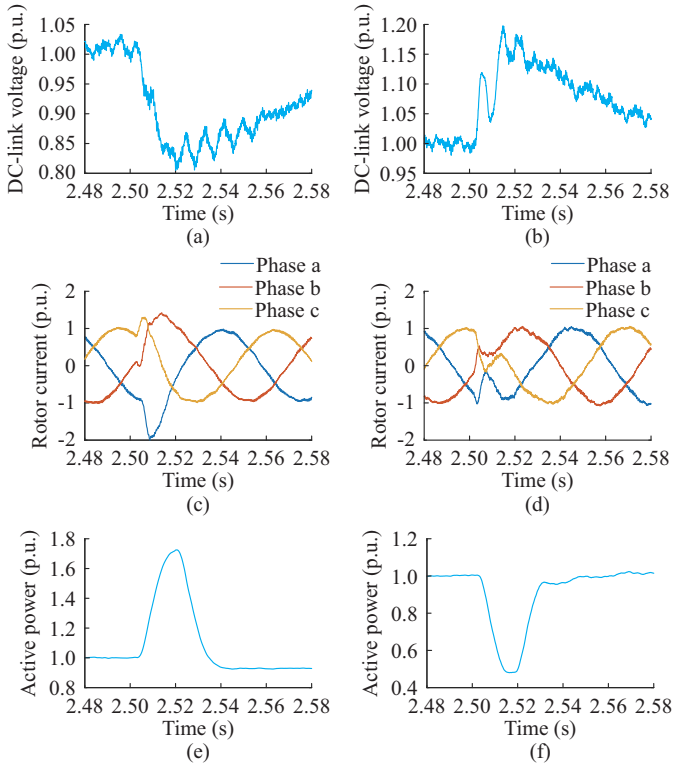

Fig. 16. Dynamic behavior of equivalent WPP during loss of a line. (a) DC-link voltage with negative phase-angle jump. (b) DC-link voltage with positive phase-angle jump. (c) Rotor current with negative phase-angle jump. (d) Rotor current with positive phase-angle jump. (e) Active power with negative phase-angle jump. (f) Active power with positive phase-angle jump.

In this case, the phase-angle jump is negative, which leads to an undervoltage of 0.8 p.u. at the beginning of this event. The voltage increases from 0.8 p.u. to 0.95 p.u. between 2.52 s and 2.58 s. The rotor current shows an overcurrent of 2 p.u. in the negative peak and 1.3 p.u. in the positive peak immediately after the loss of the line, respectively. The rotor

currents return to the pre-event value after the event. The active power shows an overshoot close to 1.7 p.u. at the beginning of the event. After the loss of the line, the active power goes to 0.9 p.u..

Figure 16(b), (d), and (f) shows the results for the loss of a line, which leads to a positive phase-angle jump. In this case, the DC-link voltage shows an overvoltage of 1.2 p.u. at the beginning of this event, and the voltage recovers from 0.8 p.u. to 0.95 p.u. between 2.52 s and 2.58 s. The rotor current shows an undercurrent immediately after the loss of the line and returns to the pre-event value after the event. It causes an undershoot in active power of 0.5 p.u.. After the loss of the line, the active power returns to a value close to unity.

E. Voltage Dips due to Transformer Energizing

Figure 17 presents the dynamic behavior of the equivalent WPP during the transformer energizing from Fig. 9.

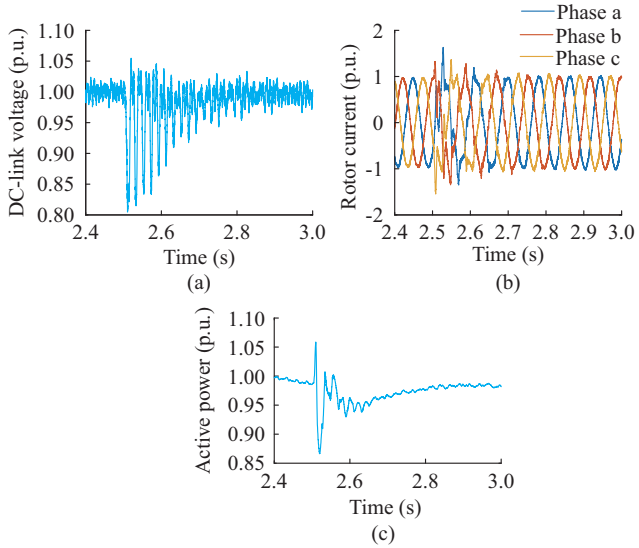

Fig. 17. Dynamic behavior of equivalent WPP during transformer energizing. (a) DC-link voltage. (b) Rotor current. (c) Active power.

The DC-link voltage shows an oscillation between 0.8 p.u. and 1.05 p.u. during the voltage dip. Similar to the asymmetrical dips caused by faults, the cause of this oscillation is related to the imbalance among the phases. However, the DC-voltage oscillation differs from the asymmetrical dip caused by a fault, because the DC-link voltage follows the "envelop" of the RMS voltage dip. In other words, the DC-link oscillation is related to the slow recovery of the transformer energizing.

The rotor voltage component induced by the negative-sequence voltage component also results in large current ripples through the rotor windings. In this case, the rotor current presents an overshoot of 1.5 p.u.. The heavy harmonic distortion is also visible in the rotor current. In this case, the waveform is more distorted in the peaks, which is a common effect of even harmonics.

The active power shows an overshoot of 1.05 p.u. at the beginning of the voltage dip. During the dip, the active power is reduced proportionally to the dip magnitude (around 0.87 p.u.). As the recovery process for the transformer energizing is slow, the DFIG takes more time to recover to the pre-dip values.

F. Voltage Transients due to Capacitor Switching

Figure 18 presents the dynamic behavior of the equivalent WPP during the capacitor switching from Fig. 10.

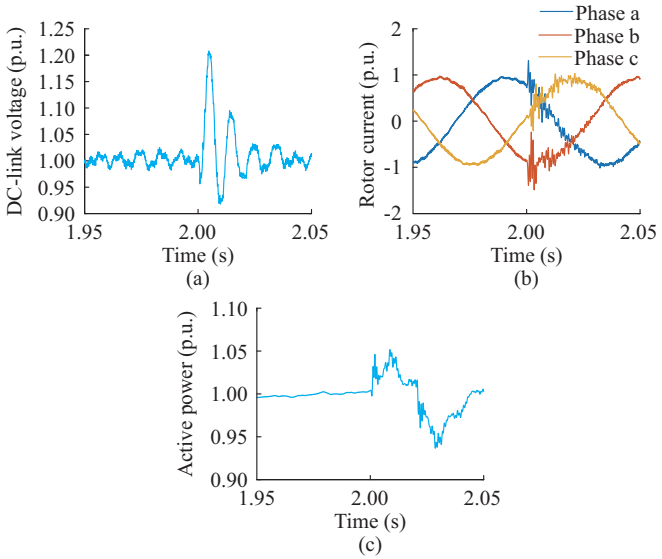

Fig. 18. Dynamic behavior of equivalent WPP during capacitor switching. (a) DC-link voltage. (b) Rotor current. (c) Active power.

As the transient from the transmission system is amplified, the DC-link voltage shows an overshoot during the capacitor switching. In this case, the overvoltage of the DC link reaches 1.2 p.u.. The duration of this overvoltage is the same as that of the transient. The rotor current shows an overcurrent and a transient during the capacitor bank switching. The active power shows three stages during the transient: overshoot of 1.05 p.u., reduction to 0.95 p.u., and recovery to the pre-transient power.

G. Voltage Transients due to Cable Switching

Figure 19 presents the dynamic behavior of the equivalent WPP during the cable switching from Fig. 11.

Similar to the capacitor bank switching, the DC-link voltage shows an overshoot at the beginning of the transient, which is proportional to the overvoltage at the WT terminals. The rotor current also shows a transient during the cable switching. The active power presents small oscillations related to the voltage transient. In this case, the active power oscillates between 0.99 p.u. and 1.02 p.u.. The active power after the transient does not return exactly to the pre-transient value, because the voltage magnitude is slightly higher after the cable switching.

H. Voltage Dips due to GIC

Figure 20 presents the dynamic behavior of the equivalent WPP during the GIC from Fig. 6. The dynamic behavior is similar to the behavior during transformer energizing. The DC-link voltage shows an oscillation with an "envelop" shape following the transformer saturation. The rotor current shows an increased value and harmonic distortion, especially during the peaks. Besides, the active power changes accordingly to the voltage at the WT terminals.

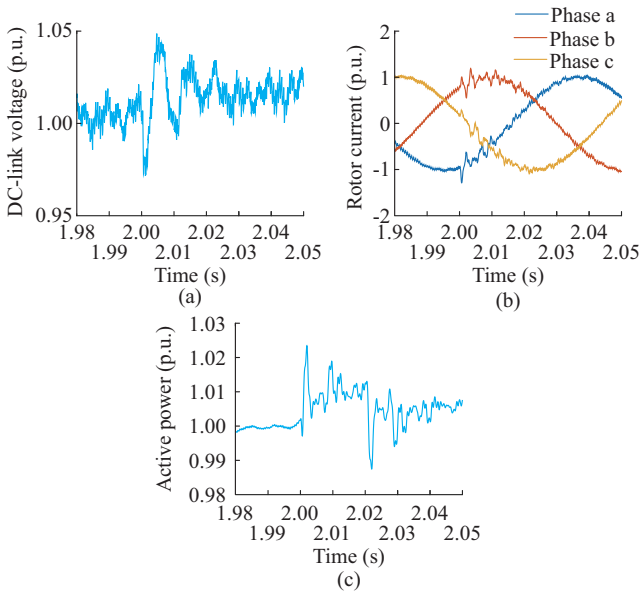

Fig. 19. Dynamic behavior of equivalent WPP during cable switching. (a) DC-link voltage. (b) Rotor current. (c) Active power.

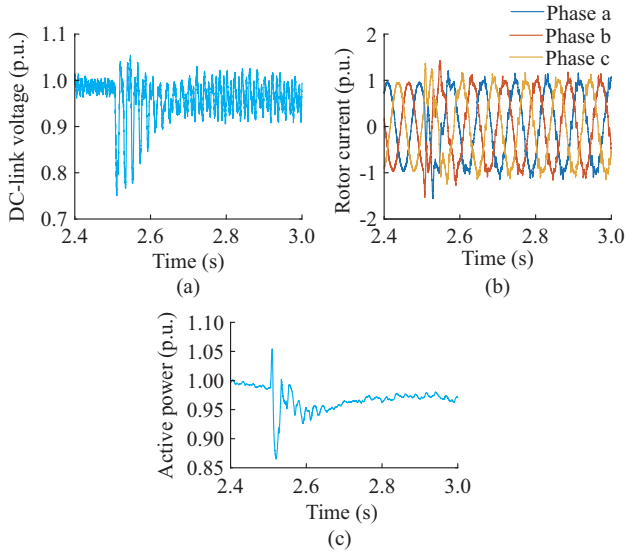

Fig. 20. Dynamic behavior of equivalent WPP during GIC. (a) DC-link voltage. (b) Rotor current. (c) Active power.

However, the GIC has a long duration and its effects are still noted in the equivalent time of recovery during the transformer energizing. The reason is that the voltage after 2.8 s for the GIC is still unbalanced. This way, after 2.8 s, the DC-link voltage still shows a small oscillation, the rotor current still contains harmonics, and the active power reaches a value lower than the pre-event value, which is lower than that during the transformer energizing.

VI. FRT Requirements in Grid Codes and Connection Agreements

Voltage dips, as defined in the FRT requirements, are a simplified version of the voltage dips as they occur in reality. There are additional characteristics of voltage dips that need to be considered in FRT studies and compliance verification. Those characteristics vary strongly between locations. Besides, the dip characteristic can differ at a same location at different moments in time. It is not always obvious which value of a characteristic should be considered as the worst case.

Including all these additional characteristics in the FRT requirements would make the requirements too complicated or even non-applicable. Therefore, we do not recommend adding additional characteristics to the actual requirements.

However, we strongly recommend adding additional guidance and recommendations to the documents containing the FRT requirements. Such guidance and recommendations should aid the wind power manufacturers in verifying and improving the FRT of WTs and WPPs.

Next to the FRT requirements for voltage dip, the grid codes should also contain requirements (including guidance and recommendations) on the FRT during other types of voltage disturbances, which include: ① voltage dips due to transformer energizing; ② transients due to switching of capacitor banks; ③ transients due to switching of long AC transmission cables; ④ phase-angle jumps without a voltage dip due to the loss of a major transmission connection; and ⑤ high levels of voltage distortion due to GIC.

VII. Recommendations for Research Community

When studying the FRT of WTs, it is very important to consider that the voltage dip as defined in the grid codes is simplified. In reality, the dip can strongly deviate from this simplified one for two reasons:

1) The voltage dip in the transmission system is not a "rectangular dip"; instead, oscillations may occur at the beginning and end of the dip, and the voltage recovery may occur in two or three steps.

2) The voltage waveform can change a lot during the propagation from the transmission system to the WT terminals.

More knowledge is needed on how the protection in WPP is impacted by a number of phenomena that occur in association with the voltage dip due to a fault, including: ① oscillations at the beginning of a voltage dip; ② oscillations at the end of a voltage dip; ③ harmonic distortion during a voltage dip; and ④ harmonic distortion after a voltage dip.

As the WPP has to ride through the voltage dip, according to the FRT requirements in the grid codes, the protection in the WPP should not trip due to any of these phenomena.

Standardized definitions are needed for voltage-dip characteristics beyond the residual voltage and duration. Complete proposals are available for phase-angle jump and imbalance during the dip. Further research is needed for other characteristics. Special emphasis should be placed on the details of dip initiation and voltage recovery.

More studies are needed after the propagation of voltage dips from the transmission system to the WT terminals in large WPPs. A wide range of resulting dips could occur based on the properties of the collection grid and the way it is connected to the transmission system. FRT studies should therefore be conducted for a range of WPPs and connections to the grid. The individual behavior of WT in distinct WPPs should also be explored. Moreover, the impact on the trans-

mission system protection should be studied.

A specific case to study is the propagation of voltage dips through an HVDC link towards a WPP. The study can cover HVDC based on thyristor or on voltage source converters (VSCs).

Studies are needed on: ① waveform distortion due to transformer saturation under geomagnetically induced currents; ② the occurrence of phase-angle jumps without voltage dips due to the loss of a major transmission link; ③ the mapping of extreme transient events and the way in which they may affect WTs and WPPs.

The simulations and modelling in this paper and in other studies on FRT consider rather typical faults and voltage dips. Common dips due to faults in the transmission system are of short duration, typically within 100 ms. The dips that are the base for the requirements on FRT are of longer duration, which is 250 ms and more. The assumption typically made is that those dips will be the same as the typical ones, but of longer duration. Insufficient knowledge is available to determine whether this assumption is correct. Studies are needed to find out which scenarios in the transmission system will result in the dimensioning dips under the FRT requirements. Next, studies are needed to find out the details of the resulting dips.

VIII. Conclusion

Not only voltage dips caused by electrical faults should be considered while assessing the FRT of WPP, but the voltage dips caused by transformer energizing, transients caused by capacitor switching, cable switching, and GIC should also be considered.

The models of voltage disturbances without considering the transfer to WTs terminals are not suitable for detailed studies. The disturbances originating inside the WPP do not fall under the realm of FRT but under the realm of power system protection.

The voltage dips caused by electrical faults are not rectangular. There are oscillations at the beginning and the end of the voltage dips. The transients at the beginning of the voltage dip can be amplified and last longer when propagating to the WT terminals accordingly to the resonance frequency of the collection grid. There is a need to explore in details the propagation of dips with transients in cable-dominated system.

The voltage recovery for voltage dips caused by faults may occur in more than one step. The two-stage recovery is very common in transmission systems and therefore essential to be considered in FRT studies. Each stage can impact the behavior of a WPP distinctly. The voltage recovery for voltage dips due to transformer energizing and GIC is slower than that for the fault-caused dips. The slow recovery leads to prolonged restoration of the dynamic variables of the converters and the generators.

Asymmetrical voltage dips change their types and magnitudes when propagating from the transmission system towards the WT terminals. Ignoring this fact might lead to an overestimation of the severity of the dynamic behavior. In contrast, for capacitor switching and cable switching, it might lead to underestimation of the severity of the overvoltage at the WT terminals. More studies are needed to quantify the impact of the changes in characteristics during the transfer on the severity of the dynamic behavior.

Voltage dips caused by faults, transformer-energizing, and GIC events are associated with high harmonic content. Especially, in the cases of transformer energizing and GIC, the even harmonic content is much higher than normal. Resonances in the transmission system and/or between the transmission system and the WT terminals might result in even higher levels of harmonic distortion. More studies are needed to understand the impact of these short-term harmonics on the internal protection of WPP and the power converters.

Phase-angle jumps caused by faults in the transmission cables or due to the loss of major lines/cables lead to a distinct performance of WT. Both positive and negative phase-angle jumps can occur and have a different impact on the WT, which need to be considered. More studies are needed to model the impact of phase-angle jumps on the dynamic behavior of large WPP.

This paper regards WTs as part of large WPPs and should be repeated for other equipment. The major importance for the operation security of the transmission system is the immunity of large individual installations and large numbers of small devices. This paper considers the large solar power installations, large numbers of small solar power installations, large numbers of small charging installations for electric vehicles, HVDC links, and protection of major transmission lines.

Appendix A

TABLE AI
Parameters of Equivalent WPP

Equipment	Parameter	Value
Grid	R_{grid} (Ω)	0.5760
	L_{grid} (mH)	0.0183
	S (MVA)	2500
Cable 1	R_1 (Ω)	0.434
	L_1 (mH)	3.46
	$C_1/2$ (μF)	5.90
Transformer 1	R_{T1} (Ω)	0.035
	L_{T1} (mH)	1
	Power (MVA)	4×220
Cable 2	R_2 (mΩ)	13.27
	L_2 (μH)	75.4
	$C_2/2$ (μF)	4.25
Transformer 2	R_{T2} (mΩ)	1.4
	L_{T2} (μH)	190
	Power (MVA)	42×6.5
Filter	R_F (Ω)	8.64
	L_F (mH)	1.63
	C_F (nF)	5.74
WT generator	R_G (p.u.)	2.38×10^{-6}
	L_G (p.u.)	2.38×10^{-3}

TABLE AII
CONTROL PARAMETERS OF WTS

Control parameter	Value
DC bus voltage regulator gains	$K_p = 8$, $K_i = 1000$
Grid-side converter current regulator gains	$K_p = 0.83$, $K_i = 5$
Rotor-side converter current regulator gains	$K_p = 0.6$, $K_i = 8$
Q and V regulator gains	$K_{ivar} = 0.05$, $K_{ivolt} = 20$

REFERENCES

[1] P. Kundur, *Power System Stability and Control*, New York: McGraw-Hill, 1994.

[2] C. Jauch, J. Matevosyan, T. Ackermann *et al*., "International comparison of requirements for connection of wind turbines to power systems," *Wind Energy*, vol. 8, no. 3, pp. 295-306, Jul. 2005.

[3] *Vindmøller Tilsluttet Net Med Spændinger Under 100 kV*, Energinet Technical Regulation 3.2.5, 2003.

[4] *Specifications for Connecting Wind Farms to the Transmission Networks*, Eltra, 2002.

[5] *Affärsverket Svenska Kraftnäts Föreskrifter om Driftsäkerhetsteknisk Utformning av Produktionsanläggningar*, Svenska Kraftnät, 2004.

[6] *Netzanschlussregeln*, *Hoch-und Höchstspannung*, E.ON Netz, 2003.

[7] *Guidance Note for the Connection of Wind Farms*, Scottish Hydro Electric, 2002.

[8] *Wind Farm Connection Requirements*, E. N. Grid, 2002.

[9] *Wind Turbines Connected to Grids with Voltages Above 100 kV*, Elkraft System and Eltra Technical Regulation, 2004.

[10] U. S. A. Federal Energy Regulatory Commission. (2005, Dec.). Interconnection for wind energy. [Online]. Available: https://www. federalregister. gov/documents/2005/12/19/05-24173/interconnection-for-wind-energy.

[11] NORDEL. (2004, Dec.). Nordic grid code. [Online]. Available: http://webhotel2. tut. fi/units/set/research/adine/materiaalit/Active% 20network/System%20integration/Grid%20codes/Nordel%20grid%20code%202007-00129-01-E.pdf

[12] *Establishing a Network Code on Requirements for Grid Connection of Generators*, Commission Regulation (EU), 2016.

[13] *Wind Energy Generation Systems–Part 21-1: Measurement and Assessment of Electrical Characteristics–Wind Turbines*, IEC standard 61400-21-1, 2019.

[14] *Wind Turbines – Part 27-1: Electrical Simulation Models – Wind Turbines*, IEC Standard 61400-27-1, 2015.

[15] *Voltage Dip Immunity of Equipment and Installations*, W. Group and C4.110, 2010.

[16] *Recommended Practice for Voltage Sag and Short Interruption Ride-through Testing for End-use Electrical Equipment Rated Less Than 1000 V*, IEEE Standard 1668, 2017.

[17] M. H. J. Bollen, G. Olguin, and M. Martins, "Voltage dips at the terminals of wind power installations," *Wind Energy*, vol. 8, no. 3, pp. 307-318, Jul. 2005.

[18] J. Lopez, P. Sanchis, X. Roboam *et al*., "Dynamic behavior of the doubly fed induction generator during three-phase voltage dips," *IEEE Transactions on Energy Conversion*, vol. 22, no. 3, pp. 709-717, Sept. 2007.

[19] J. Lopez, E. Gubia, P. Sanchis *et al*., "Wind turbines based on doubly fed induction generator under asymmetrical voltage dips," *IEEE Transactions on Energy Conversion*, vol. 23, no. 1, pp. 321-330, Mar. 2008.

[20] M. Mohseni, S. M. Islam, and M. A. S. Masoum, "Impacts of symmetrical and asymmetrical voltage sags on DFIG-based wind turbines considering phase-angle jump, voltage recovery, and sag parameters," *IEEE Transactions on Power Electronics*, vol. 26, no. 5, pp. 1587-1598, May 2011.

[21] A. Rolán, J. Pedra, and F. Córcoles, "Detailed study of DFIG-based wind turbines to overcome the most severe grid faults," *International Journal of Electrical Power and Energy Systems*, vol. 62, pp. 868-878, Nov. 2014.

[22] G. Wen, Y. Chen, Z. Zhong *et al*., "Dynamic voltage and current assignment strategies of nine-switch-converter-based DFIG wind power system for low-voltage ride-through (LVRT) under symmetrical grid voltage dip," *IEEE Transactions on Industrial Applications*, vol. 52, no. 4, pp. 3422-3434, Jul.-Aug. 2016.

[23] M. Molinas, J. A. Suul, and T. Undeland, "Low voltage ride through of wind farms with cage generators: STATCOM versus SVC," *IEEE Transactions on Power Electronics*, vol. 23, no. 3, pp. 1104-1117, May 2008.

[24] K. Kim, Y. Jeung, D. Lee *et al.*, "LVRT scheme of PMSG wind power systems based on feedback linearization," *IEEE Transactions on Power Electronics*, vol. 27, no. 5, pp. 2376-2384, May 2012.

[25] S. Alepuz, S. Busquets-Monge, J. Bordonau *et al*., "Control strategies based on symmetrical components for grid-connected converters under voltage dips," *IEEE Transactions on Industrial Electronics*, vol. 56, no. 6, pp. 2162-2173, Jun. 2009.

[26] H. M. Yassin, H. H. Hanafy, and M. M. Hallouda, "Enhancement low-voltage ride through capability of permanent magnet synchronous generator-based wind turbines using interval type-2 fuzzy control," *IET Renewable Power Generation*, vol. 10, no. 3, pp. 339-348, Mar. 2016.

[27] I. Ngamroo and T. Karaipoom, "Cooperative control of SFCL and SMES for enhancing fault ride through capability and smoothing power fluctuation of DFIG wind farm," *IEEE Transactions on Applied Superconductivity*, vol. 24, no. 5, pp. 1-4, Oct. 2014.

[28] G. D. Marques and D. M. Sousa, "Understanding the doubly fed induction generator during voltage dips," *IEEE Transactions on Energy Conversion*, vol. 27, no. 2, pp. 421-431, Jun. 2012.

[29] R. Sadeghi, S. M. Madani, T. A. Lipo *et al*., "Voltage-dip analysis of brushless doubly fed induction generator using reduced T-model," *IEEE Transactions on Industrial Electronics*, vol. 66, no. 10, pp. 7510-7519, Oct. 2019.

[30] A. O. Ibrahim, T. H. Nguyen, D. Lee *et al.*, "A fault ride-through technique of DFIG wind turbine systems using dynamic voltage restorers," *IEEE Transactions on Energy Conversion*, vol. 26, no. 3, pp. 871-882, Sept. 2011.

[31] J. Yang, J. E. Fletcher, and J. O'Reilly, "A series-dynamic-resistor-based converter protection scheme for doubly-fed induction generator during various fault conditions," *IEEE Transactions on Energy Conversion*, vol. 25, no. 2, pp. 422-432, Jun. 2010.

[32] Y. M. Alsmadi, L. Xu, F. Blaabjerg *et al.*, "Detailed investigation and performance improvement of the dynamic behavior of grid-connected DFIG-based wind turbines under LVRT conditions," *IEEE Transactions on Industrial Applications*, vol. 54, no. 5, pp. 4795-4812, Sep.-Oct. 2018.

[33] S. Swain and P. K. Ray, "Short circuit fault analysis in a grid connected DFIG based wind energy system with active crowbar protection circuit for ridethrough capability and power quality improvement," *International Journal of Electrical Power and Energy Systems*, vol. 84, pp. 64-75, Jan. 2017.

[34] Z. Zheng, C. Huang, R. Yang *et al.*, "A low voltage ride through scheme for DFIG-based wind farm with SFCL and RSC control," *IEEE Transactions on Applied Superconductivity*, vol. 29, no. 2, pp. 1-5, Mar. 2019.

[35] A. M. Rauf, V. Khadkikar, and M. S. El Moursi, "A new fault ride-through (FRT) topology for induction generator based wind energy conversion systems," *IEEE Transactions on Power Delivery*, vol. 34, no. 3, pp. 1129-1137, Jun. 2019.

[36] B. Li, J. Liu, X. Wang *et al*., "Fault studies and distance protection of transmission lines connected to DFIG-based wind farms," *Applied Sciences*, vol. 8, p. 562, Apr. 2018.

[37] M. Firouzi and G. B. Gharehpetian, "LVRT performance enhancement of DFIG-based wind farms by capacitive bridge-type fault current limiter," *IEEE Transactions on Sustainable Energy*, vol. 9, no. 3, pp. 1118-1125, Jul. 2018.

[38] M. M. Kyaw and V. K. Ramachandaramurthy, "Fault ride through and voltage regulation for grid connected wind turbine," *Renewable Energy*, vol. 36, no. 1, pp. 206-215, Jan. 2011.

[39] N. Jelani and M. Molinas, "Asymmetrical fault ride through as ancillary service by constant power loads in grid-connected wind farm," *IEEE Transactions on Power Electronics*, vol. 30, no. 3, pp. 1704-1713, Mar. 2015.

[40] H. Geng, C. Liu, and G. Yang, "LVRT capability of DFIG-based WECS under asymmetrical grid fault condition," *IEEE Transactions on Industrial Electronics*, vol. 60, no. 6, pp. 2495-2509, Jun. 2013.

[41] F. Xiao, Z. Zhang, and X. Yin, "Fault current characteristics of the DFIG under asymmetrical fault conditions," *Energies*, vol. 8, pp. 10971-10992, Sept. 2015.

[42] J. Mohammadi, S. Afsharnia, S. Vaez-Zadeh *et al.*, "Improved fault ride through strategy for doubly fed induction generator based wind turbines under both symmetrical and asymmetrical grid faults," *IET Renewable Power Generation*, vol. 10, no. 8, pp. 1114-1122, Sept. 2016.

[43] K. Tahir, C. Belfedal, T. Allaoui *et al.*, "A new control strategy of WF-

SG-based wind turbine to enhance the LVRT capability," *International Journal of Electrical Power and Energy Systems*, vol. 79, pp. 172-187, Jun. 2016.
[44] S. B. Naderi, M. Negnevitsky, A. Jalilian *et al*., "Low voltage ride-through enhancement of DFIG-based wind turbine using DC link switchable resistive type fault current limiter," *International Journal of Electrical Power and Energy Systems*, vol. 86, pp. 104-119, Mar. 2017.
[45] M. M. Islam, E. Hossain, S. Padmanaban *et al*., "A new perspective of wind power grid codes under unbalanced and distorted grid conditions," *IEEE Access*, vol. 8, pp. 15931-15944, Jan. 2020.
[46] M. F. M. Arani and Y. A.-R. I. Mohamed, "Assessment and enhancement of a full-scale PMSG-based wind power generator performance under faults," *IEEE Transactions on Energy Conversion*, vol. 31, pp. 728-739, Jun. 2016.
[47] A. A. van der Meer, M. Ndreko, M. Gibescu *et al.*, "The effect of FRT behavior of VSC-HVDC-connected offshore wind power plants on AC/DC system dynamics," *IEEE Transactions on Power Delivery*, vol. 31, pp. 878-887, Apr. 2016.
[48] R. Sharma, Q. Wu, S. T. Cha *et al.*, "Power hardware in the loop validation of fault ride through of VSC HVDC connected offshore wind power plants," *Journal of Modern Power Systems and Clean Energy*, vol. 2, no. 1, pp. 23-29, Mar. 2014.
[49] A. Moawwad, M. S. El Moursi, and W. Xiao, "Advanced fault ride-through management scheme for VSC-HVDC connecting offshore wind farms," *IEEE Transactions on Power Systems*, vol. 31, no. 6, pp. 4923-4934, Nov. 2016.
[50] N. G. Z. Espinoza, M. Bongiorno, and O. Carlson, "Novel LVRT testing method for wind turbines using flexible VSC technology," *IEEE Transactions on Sustainable Energy*, vol. 6, no. 3, pp. 1140-1149, Jul. 2015.
[51] W.-T. Liu, Y.-K. Wu, C.-Y. Lee *et al*., "Effect of low-voltage-ride-through technologies on the first taiwan offshore wind farm planning," *IEEE Transactions on Sustainable Energy*, vol. 2, pp. 78-86, Oct. 2011.
[52] I. Babaeiyazdi, M. Rezaei-Zare, and A. Rezaei-Zare, "Wind farm operating conditions under geomagnetic disturbance," *IEEE Transactions on Power Delivery*, vol. 35, no. 3, pp. 1357-1364, Jun. 2020.
[53] I. Arana, A. Hernandez, G. Thumm *et al*., "Energization of wind turbine transformers with an auxiliary generator in a large offshore wind farm during islanded operation," *IEEE Transactions on Power Delivery*, vol. 26, no. 4, pp. 2792-2800, Oct. 2011.
[54] Y. Wang, M. H. J. Bollen, and X. Xiao, "Calculation of the phase-angle-jump for voltage dips in three-phase systems," *IEEE Transactions on Power Delivery*, vol. 30, no. 1, pp. 480-487, Feb. 2015.
[55] Y. Wang, A. Bagheri, M. H. J. Bollen *et al.*, "Single-event characteristics for voltage dips in three-phase systems," *IEEE Transactions on Power Delivery*, vol. 32, no. 2, pp. 832-840, Apr. 2017.
[56] Y. Wang, X. Xiao, and M. H. J. Bollen, "Challenges in the calculation methods of point-on-wave characteristics for voltage dips," in *Proceedings of 2016 17th International Conference on Harmonics and Quality of Power (ICHQP)*, Belo Horizonte, Brazil, Oct. 2016, pp. 513-517.
[57] D. Schwanz, M. Bollen, and A. Larsson, "Secondary harmonic emission in wind power plants," in *Proceedings of 2019 IEEE PowerTech Conference*, Milan, Italy, Jun. 2019, pp. 1-6.
[58] E. Muljadi, C. P. Butterfield, A. Ellis *et al.*, "Equivalencing the collector system of a large wind power plant," in *Proceedings of 2006 IEEE Power Engineering Society General Meeting*, Montreal, Canada, Jun. 2006, pp. 1-9.
[59] N. W. Miller, J. J. Sanchez-Gasca, W. W. Price *et al.*, "Dynamic modeling of GE 1.5 and 3.6 MW wind turbine-generators for stability simulations," in *Proceedings of 2003 IEEE Power Engineering Society General Meeting*, Toronto, Canada, Jul. 2003, pp. 1977-1983.
[60] O. Lennerhag and M. H. J. Bollen, "Impact of uncertainties on resonant overvoltages following transformer energization," *Electric Power Systems Research*, vol. 187, pp. 1-10, Oct. 2020.
[61] A. Fouad, M. Elshahed, M. Sayed *et al.*, "Harmonic resonance overvoltage due to main transformer energization in large wind farms, Zafarana, Egypt," *Ain Shams Engineering Journal*, vol. 10, pp. 731-743, Dec. 2019.
[62] T. Ohno, C. L. Bak, A. Ametani *et al.*, "Statistical distribution of energization overvoltages of EHV cables," *IEEE Transactions on Power Delivery*, vol. 28, no. 3, pp. 1423-1432, Jul. 2013.
[63] A. Ametani, T. Ohno, N. Nagaoka *et al.*, *Cable System Transients: Theory, Modeling and Simulation*, Singapore: John Wiley & Sons, 2015.
[64] *Geomagnetic Disturbances (GMD) Impacts on Protection Systems*, IEEE PES Technical Report PES-TR72, 2019.
[65] *Understanding of Geomagnetic Storm Environment for High Voltage Power Grids*, CIGRE Technical Brochure TB-780, 2019.

Roger Alves de Oliveira received his bachelor's degree of electrical engineering in 2014 from Federal Institute of Technology, Science and Education (IFSul), Pelotas, Brazil. He received the M. Sc. degree from Federal University of Rio Grande do Sul, Porto Alegre, Brazil, in 2018. Currently, he is a Ph.D. student in the Electric Power Engineering Group at Luleå University of Technology, Skellefteå, Sweden. He was a Lecturer of power systems subjects in IFSul between 2014 and 2016. His main research interests include voltage dips, FRT of WPPs, and deep learning for large-scale power system data.

Math H. J. Bollen received the M.Sc. and Ph.D. degrees from Eindhoven University of Technology, Eindhoven, The Netherlands, in 1985 and 1989, respectively. Currently, he is Professor in electric power engineering at Luleå University of Technology, Skellefteå, Sweden. Before that, he was Lecturer at the Institute of Science and Technology, University of Manchester, Manchester, U.K., Professor in electric power systems at Chalmers University of Technology, Gothenburg, Sweden, R&D Manager and Technical Manager for power quality and distributed generation at STRI AB, Gothenburg, Sweden, and Technical Expect at the Energy Markets Inspectorate, Eskilstuna, Sweden. He has published a few hundred papers including a number of fundamental papers on voltage dip analysis, two textbooks on power quality, i.e., Understanding Power Quality Problems, and Signal Processing of Power Quality Disturbances, and two textbooks on the future power system, i.e., Integration of Distributed Generation in the Power System, and The Smart Grid – Adapting the Power System to New Challenges. He is Fellow of IEEE and recipient of the CIGRE study committee award. He has among others defined voltage dips as a research subject, spread the use of the term "hosting capacity", and contributed to defining supraharmonics as a research area. His research interests cover a broad range of power-system issues, including power quality (voltage dips, harmonics, supraharmonics, flicker and more), power system protection, power system reliability, signal-processing and machine-learning applications, integration of renewable electricity production, smart grids, and hosting-capacity calculations.